Two-Tier Cache-Aided Full-Duplex Content Delivery in Satellite–Terrestrial Networks

Quynh T. Ngo[1(✉)], Khoa T. Phan[1], Wei Xiang[1], Abdun Mahmood[1], and Jill Slay[2]

[1] School of Engineering and Mathematical Sciences, Department of Computer Science and Information Technology, La Trobe University, Melbourne, Australia
{T.Ngo,K.Phan,W.Xiang,A.Mahmood}@latrobe.edu.au
[2] School of Computer and Information Science, University of South Australia, Adelaide, Australia
Jill.Slay@unisa.edu.au

Abstract. Enabling global Internet access is challenging for the Internet of Things due to limited range of terrestrial network services. One viable solution is to deploy satellites into terrestrial systems for coverage extension. However, operating a hybrid satellite-terrestrial system incurs potentially high satellite bandwidth consumption and excessive service latency. This work aims to reduce the content delivery delay and bandwidth consumption from the Internet-connected gateway to remote users in satellite terrestrial networks, using a two-tier cache-enabled full-duplex system model where content caches are placed at the satellite and the ground station. A closed-form solution for successful delivery probability of content files within allocated time slot under general caching policy is derived considering the requested content distributions and channel statistics. Illustrative results demonstrate superior performance of the proposed system over those of single-tier cache-aided. The trade-off between successful delivery probability and satellite bandwidth consumption, in addition to insights on the network support ability are also investigated.

Keywords: Satellite-terrestrial networks · Edge caching · Full-duplex · Successful delivery probability · Cache placement design

1 Introduction

Although being around for many years, cellular-based technologies for the Internet of Things (IoT) have not fulfilled the demand of globally connecting everyone and everything. To offer service across all geographic regions, particularly, in rugged or dispersed terrain, integrating satellites into IoT networks has been proposed. Providing better service reliability and coverage, satellite is a more effective solution for IoT than cellular network. Embedding satellite into IoT

D. Mohaisen and R. Jin (Eds.): CSoNet 2021, LNCS 13116, pp. 291–302, 2021.
https://doi.org/10.1007/978-3-030-91434-9_26

networks, however, poses challenges in service delays and satellite bandwidth cost. A content delivered to end-users from the Internet-connected gateway is relayed through satellite(s) and ground station(s), which extends the serving time in addition to very pricey and often limited satellite bandwidth. Excessive content delivery delay can hinder potential use of satellite IoT systems to support delay-sensitive applications. To address with these challenges, caching has been proposed to move content storage to the edge devices closer to the users. Caching popular contents at the network edge can reduce network congestion and decrease content delivery latency [12].

Employing edge caching technique in hybrid satellite-terrestrial relay networks, [2] proposes an amplify and forward relaying protocols where the cache is enabled at relays on the ground (a.k.a. ground stations in our current work). The work in [2] considers the most popular and uniform content-based cache placement schemes, that shows substantial improvement over the traditional approach without caching in terms of outage probability. To off-load the backhaul of terrestrial network, [9] proposes using the hybrid satellite terrestrial network in combination with an off-line edge caching algorithm. The performance of the proposed off-line caching algorithm is measured through cache hit ratio. Using the same network model as in [9,13] investigates the system performance in two use cases: in dense urban areas and in sparsely populated regions. The effectiveness of the system is studied through cache hit ratio and cost per bit for satellite transmission. It should be emphasized that [2,9,13] consider dual-hop downlink satellite–relay(s)–users transmissions with single-tier cache placed at the relays. The satellite uplink communications from the Internet-connected gateway to the satellite is not considered, which is usually the bottleneck in satellite IoT systems due to large bandwidth consumption.

Aiming at reducing the satellite uplink bandwidth consumption, additional caching at the satellite has been proposed. The work [15] proposes a two-tier caching model where the first and second cache tiers are placed in the ground stations, and in the satellite, respectively. Caches at each ground station are used for the popular contents in its local area, while the satellite's cache is used for the most popular contents in its coverage (containing multiple ground stations) to take advantage of the satellite's broadcast nature to the ground stations. Non-cached contents can be retrieved from the gateway if needed. While [15] aims to minimize the satellite bandwidth consumption, the file delivery time, a critical concern in satellite IoT operation, is not investigated that requires more elaborated analysis.

In this paper, we consider a two-tier cache-aided model in hybrid satellite-terrestrial systems [15] considering end-to-end gateway to end-users data transmissions over realistic channel models. Our work focuses on the content delivery time analysis in terms of successful delivery probability (SDP) considering full-duplex (FD) transmissions at the satellite and ground station, albeit with imperfect self-interference cancellation (SIC). Deploying FD communications will potentially shorten the service delivery time comparing to half-duplex mode providing sufficiently effective SIC, and hence, increasing the SDP. A closed-

form expression for the SDP under FD mode is derived taking into account the requested content characteristics, channel statistics, and network configurations. The results enable convenient evaluations of the trade-off between SDP and satellite bandwidth consumption. Numerical results are presented for the network performance behavior under two caching policies: uniform caching and popular caching. They also show the proposed system's merits over single-tier cache systems [2,9,13] in both SDP and satellite bandwidth consumption.

2 System Model

The satellite assisted IoT system composes of a satellite S, an Internet connected satellite gateway G, a ground station G_s and a set of K end-users $U_i, i = 1, \ldots, K$ as depicted in Fig. 1. In this system, S is a geosynchronous equatorial orbit (GEO) satellite; G_s is a low power IoT base station equipped with a satellite receiver. Both S and G_s are cache enabled. End-users U_i are IoT devices on the ground. Assuming there is no direct link from users U_i to satellite S and from the ground station to gateway due to weather factors, long distance, and/or heavy shadowing.

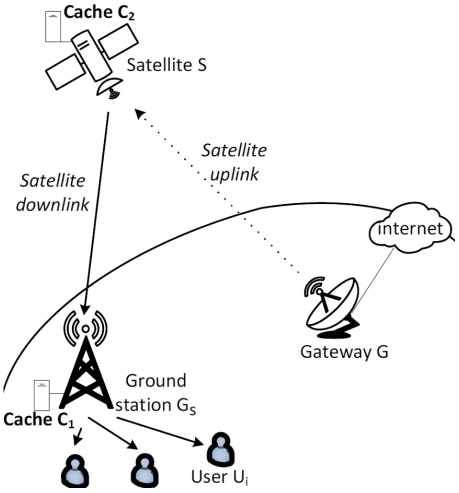

Fig. 1. Satellite IoT networks architecture.

2.1 Two-Tier Caching Model

The caching model consists of two tiers: the first tier is at the ground station with storage capacity of C_1 (bits) and the second tier is at the satellite with storage capacity of C_2 (bits). Gateway is connected to the Internet and hosts N files $W_1, \ldots, W_N$, which are assumed to be equal size of F (bits). This assumption is

for scenario of heterogeneous IoT applications. For other IoT applications, the analysis in Sects. 3, 4 and 5 can be easily extended to unequal file size. A typical caching protocol consists of two phases: the placement of files into caches and the delivery of files to users. The focus of this work is on the performance analysis of the content delivery phase. Cache placement design for content placement phase will be discussed later in the text.

The probability for a file W_n being requested follows Zipf distribution, which is $q_n = \frac{n^{-\alpha}}{\Sigma_{m=1}^{N} m^{-\alpha}}$ where $0 < \alpha < 1$ denotes the Zipf skewness factor [4]. A large α means the requests on the high popularity files, whereas a small α is related to the requests with heavy-tailed popularity. Without loss of generality, we have assumed that files $W_1, \ldots, W_N$ have decreasing popularity.

2.2 Channel Model

Consider block-based communications where a transmission section is accomplished within a coherence time T (seconds). Both large-scale fading and small-scale fading are considered. The large-scale fading is modeled by the distance-dependent power-law path-loss attenuation $d_{m-n}^{-\alpha_i}$ where d_{m-n} denotes the distance between nodes m and n, and α_i represents the path-loss exponent. For small-scale fading, the channel model proposed in [1] has been commonly used for satellite terrestrial communications [2,3,7], and Rayleigh fading channel is commonly used for terrestrial wireless communications.

The Satellite-Terrestrial Links have multipath fading and shadow fading. The multipath fading composes of one line-of-sight (LOS) and many weak scatter components. The shadow fading composes of the LOS shadow fading and multiplicative shadow fading. The channel power gain of the satellite-terrestrial links $h_{S-G_s}(t)$ has the probability distribution function (PDF) of $f_{h_{S-G_s}}(x)$ given by [1,3] as:

$$f_{h_{S-G_s}}(x) = \left(\frac{b_{1,0}m_1}{b_{1,0}m_1 + \Omega_1}\right)^{m_1} \frac{1}{b_{1,0}} \exp\left(-\frac{x}{b_{1,0}}\right) {}_1F_1\left(m_1, 1, \frac{\Omega_1 x}{b_{1,0}(b_{1,0}m_1 + \Omega_1)}\right), x \geq 0 \quad (1)$$

where $b_{1,0}$ represents the average power of the scatter components; Ω_1 represents the average power of the LOS component; m_1 is the Nakagami parameter; ${}_1F_1(.,.,.)$ is the confluent hypergeometric function [6, Eq.(9.210.1)].

The Terrestrial Links are modeled as Rayleigh fading channels with channel power gain $h_{G_s-U_i}(t)$ having the PDF given by

$$f_{h_{G_s-U_i}}(x) = \frac{1}{\bar{h}_i} \exp\left(-\frac{x}{\bar{h}_i}\right), x \geq 0 \quad (2)$$

with $\bar{h}_i$ is the average channel power gains taking into effects of small-scale fading.

Note that we have omitted the time-dependent index due to stationarity assumption.

2.3 Transmission Scheme

When caching IoT data, it is essential to maintain the data freshness [14]. This model assumes that the users will be served in a time-division multiple access (TDMA) manner which allows each user to be consecutively active in T/K (seconds). The time slot T/K will be large enough to ensure the data freshness in practical IoT applications. Under TDMA, inter-user interference does not exist. Both satellite and ground station are operating in FD mode. When channel state information is known at the transmitter, rate adaption is employed, the achievable rates (bps) on the links are

$$\begin{aligned} R_{G_s-U_i} =& B_{G_s-U_i} \log_2 \left(1 + \frac{P_{G_s}|h_{G_s-U_i}|^2 d_{G_s-U_i}^{-\alpha_g}}{\sigma^2}\right), \\ R_{S-G_s} =& B_{S-G_s} \log_2 \left(1 + \frac{P_S|h_{S-G_s}|^2 d_{S-G_s}^{-\alpha_s}}{I_{G_s} + \sigma^2}\right), \\ R_{G-S} =& B_{G-S} \log_2 \left(1 + \frac{P_G|h_{G-S}|^2 d_{G-S}^{-\alpha_s}}{I_S + \sigma^2}\right), \end{aligned} \tag{3}$$

where B_{G-S}, B_{S-G_s} and $B_{G_s-U_i}$ are the bandwidths (Hz) of the satellite uplink, downlink and the terrestrial downlink, respectively; P_S, P_G, and P_{G_s} denote the transmit powers of satellite, gateway and ground station, respectively; σ^2 is the additive white Gaussian noise power; I_S and I_{G_s} represent the residual self-interference power at the satellite and ground station, respectively, which are assumed to be proportional to the transmit power P_S and P_{G_s} with coefficient $\beta \geq 0$ being the SIC quality parameter.

When a user requests file W_n, the gateway needs to transfer the non-cached $(1 - \mu_1^n - \mu_2^n)$ portion to the satellite, which also needs to send accumulated $(1-\mu_1^n)$ portion to the ground station. By employing the FastForward protocol [5] with FD mode at the satellite, the completion time is

$$\max\left\{(1 - \mu_1^n - \mu_2^n)F/R_{G-S}, (1 - \mu_1^n)F/R_{S-G_s}\right\}.$$

Similarly, by deploying FastForward protocol with FD mode at the ground station, the (end-to-end) delivery time for transferring the whole file to the user is determined by the time for sending the $(1 - \mu_1^n)$ portion over the satellite downlink to the ground station and the time for sending the whole file over the terrestrial link to the user, that is:

$$t_{n,i} = \max\left(\frac{F}{R_{G_s-U_i}}, \frac{(1 - \mu_1^n)F}{R_{S-G_s}}, \frac{(1 - \mu_1^n - \mu_2^n)F}{R_{G-S}}\right). \tag{4}$$

Note that we have neglected the propagation delays for simplicity. Otherwise, they can be straightforwardly included in the delivery time expression as approximate constants and the mathematical derivations in the next Section remain unchanged.

3 Successful Delivery Probability

The successful delivery probability of serving a requested file to a user is defined as the probability that user receives the file within the user's active time slot. Assume that $K \ll N$, i.e., the library size is much larger than the number of users. It implies in this work that users request different files. In general, when users request similar files, more efficient delivery mechanism can be developed utilizing the broadcasting. However, it is out of the scope of this work. The following analysis is for user U_i requesting file W_n, and is true for all other users. The SDP of file W_n requested by user U_i is:

$$\psi_{n,i} = \mathbf{Pr}\left(t_{n,i} \leq \frac{T}{K}\right) \tag{5}$$

The probability operator is taken with respect to the channel power gain variables. The closed-form expression for $\psi_{n,i}$ is

$$\begin{aligned}\psi_{n,i}(\mu_1^n, \mu_2^n) &= \exp\left(-\frac{2^{\frac{FK}{\overline{TB}_{G_s-U_i}}}-1}{\overline{\gamma_1}}\right) \\ &\times \left(1 - \sum_{k=0}^{m_1-1}\sum_{q=0}^{\infty} \frac{(-1)^k}{(k!)^2}.\frac{\Gamma(1-m_1+k)}{\Gamma(1-m_1)}.\frac{\alpha_1\delta_1^k(\delta_1-\chi_1)^q}{l_1^{(q+k+1)}}.\frac{(2^{\frac{FK}{\overline{TB}_{S-G_s}}(1-\mu_1^n)}-1)^{q+k+1}}{q!(q+k+1)}\right) \\ &\times \left(1 - \sum_{k=0}^{m_2-1}\sum_{q=0}^{\infty} \frac{(-1)^k}{(k!)^2}.\frac{\Gamma(1-m_2+k)}{\Gamma(1-m_2)}.\frac{\alpha_2\delta_2^k(\delta_2-\chi_2)^q}{l_2^{(q+k+1)}}.\frac{(2^{\frac{FK}{\overline{TB}_{G-S}}(1-\mu_1^n-\mu_2^n)}-1)^{q+k+1}}{q!(q+k+1)}\right).\end{aligned} \tag{6}$$

Note that the distances between nodes in (3) are constants. Since S is a GEO satellite, all the nodes in the system have fixed locations.

Proof. Let denote:

$\gamma_1 = \frac{P_{G_s}|h_{G_s-U_i}|^2 d_{G_s-U_i}^{-\alpha_g}}{\sigma^2}, \gamma_2 = \frac{P_S|h_{S-G_s}|^2 d_{S-G_s}^{-\alpha_s}}{I_{G_s}+\sigma^2}$, and $\gamma_3 = \frac{P_G|h_{G-S}|^2 d_{G-S}^{-\alpha_s}}{I_S+\sigma^2}$.

Following (2), the PDF of γ_1 is $f_{\gamma_1}(x) = \frac{e^{-\frac{x}{\overline{\gamma_1}}}}{\overline{\gamma_1}}, \overline{\gamma_1} = \frac{P_{G_s} d_{G_s-U_i}^{-\alpha_g} \bar{h}_i}{\sigma^2}$ for $x \geq 0$.

Let denote $\alpha_1 = \left(\frac{b_{1,0}m_1}{b_{1,0}m_1+\Omega_1}\right)^{m_1} \frac{1}{b_{1,0}}$, $\chi_1 = \frac{1}{b_{1,0}}, \delta_1 = \frac{\Omega_1}{b_{1,0}(b_{1,0}m_1+\Omega_1)}$ (refer to (1)), the PDF of γ_2 is $f_{\gamma_2}(x) = \frac{\alpha_1}{l_1} e^{\frac{\delta_1-\chi_1}{l_1}x} . \sum_{k=0}^{m_1-1} \frac{(-1)^k(1-m_1)_k(\frac{\delta_1}{l_1}x)^k}{(k!)^2}$, where $l_1 = \frac{P_S d_{S-G_s}^{-\alpha_s}}{I_{G_s}+\sigma^2}$, $(.)_k$ denotes the Pochhammer symbol with $(1-m_1)_k = \frac{\Gamma(1-m_1+k)}{\Gamma(1-m_1)}$. Similarly, the PDF of γ_3 is $f_{\gamma_3}(x) = \frac{\alpha_2}{l_2} e^{-\frac{\chi_2}{l_2}x} . {}_1F_1(m_2; 1; \frac{\delta_2}{l_2}x)$ where m_2, α_2, χ_2, δ_2 are corresponding denotations in the PDF $f_{\gamma_2}(x)$; and $l_2 = \frac{P_G d_{G-S}^{-\alpha_s}}{I_S+\sigma^2}$.

Substituting (4) into (5) we have

$$\begin{aligned}\psi_n =&\mathbf{Pr}\left(\max\left(\frac{F}{R_{G_s-U_i}},\frac{(1-\mu_1^n)F}{R_{S-G_s}},\frac{(1-\mu_1^n-\mu_2^n)F}{R_{G-S}}\right)\le\frac{T}{K}\right)\\ =&\underbrace{\mathbf{Pr}\left(\frac{F}{B_{G_s-U_i}\log_2(1+\gamma_1)}\le\frac{T}{K}\right)}_{A_1}\cdot\underbrace{\mathbf{Pr}\left(\frac{(1-\mu_1^n)F}{B_{S-G_s}\log_2(1+\gamma_2)}\le\frac{T}{K}\right)}_{A_2}\\ &\cdot\underbrace{\mathbf{Pr}\left(\frac{(1-\mu_1^n-\mu_2^n)F}{B_{G-S}\log_2(1+\gamma_3)}\le\frac{T}{K}\right)}_{A_3}.\end{aligned}$$

Since γ_1 follows exponential distribution, A_1 can be directly obtained as $A_1 = \exp\left(-\frac{2^{\frac{FK}{TB_{G_s-U_i}}}-1}{\overline{\gamma_1}}\right)$. A_2 and A_3 can be obtained in the same approach as follows $A_2 = \mathbf{Pr}\left(\frac{(1-\mu_1^n)F}{B_{S-G_s}\log_2(1+\gamma_2)}\le\frac{T}{K}\right) = 1-F_{\gamma_2}(2^{\frac{FK}{TB_{S-G_s}}(1-\mu_1^n)}-1)$, where $F_{\gamma_2}(x)$ denotes the CDF of γ_2,

$$\begin{aligned}F_{\gamma_2}(x)=&\sum_{k=0}^{m_1-1}\frac{\alpha_1}{l_1}\frac{(-1)^k(1-m_1)_k(\frac{\delta_1}{l_1})^k}{(k!)^2}\int_0^x e^{\frac{\delta_1-\chi_1}{l_1}y}y^k dy\\ =&\sum_{k=0}^{m_1-1}\sum_{q=0}^{\infty}\frac{(-1)^k(1-m_1)_k}{(k!)^2}\cdot\frac{\alpha_1\delta_1^k(\delta_1-\chi_1)^q}{l_1^{q+k+1}}\cdot\frac{x^{q+k+1}}{q!(q+k+1)}.\end{aligned}$$

($e^{\frac{\delta_1-\chi_1}{l_1}y}=\sum_{q=0}^{\infty}\frac{(\frac{\delta_1-\chi_1}{l_1})^q y^q}{q!}$ is expanded using Maclaurin series.)

The average SDP of the system is defined as the weighted sum of users' SDPs:

$$\psi(\boldsymbol{\mu}_1,\boldsymbol{\mu}_2)=\sum_{i=1}^{K}\omega_i\psi_i(\boldsymbol{\mu}_1,\boldsymbol{\mu}_2)=\sum_{i=1}^{K}\omega_i\sum_{n=1}^{N}q_n\psi_{n,i}(\mu_1^n,\mu_2^n) \tag{7}$$

with weighting coefficients $\omega_i \in (0,1)$ and $\sum_i \omega_i = 1$. In the following, w.l.o.g., assume homogeneous users with $\omega_i = 1/K$, and average channel gains $\bar{h}_i = \bar{h}_k, \forall i,k$. Thus, $\psi = \psi_i$.

4 Satellite Bandwidth Consumption

Since satellite service is more expensive, we focus on the satellite uplink and downlink bandwidth consumption during content delivery phase. Assume that the total number of requests follow Poisson distribution with an average arrival rate of $\overline{\lambda}$. Because each of all N files has some portions cached at both the satellite and the ground station, the average request arrival rate for file W_n at the two caches is the same, which is $\lambda_n = q_n\overline{\lambda}$. Let p_n denote the probability that the request for file W_n is received during time T with $p_n = \lambda_n e^{-\lambda_n T}$. The satellite

bandwidth consumption to deliver file W_n includes the downlink consumption when transmitting the cached portion of the file $p_n\mu_2^n F$, the relay portion of the file $p_n(1-\mu_1^n-\mu_2^n)F$ and the uplink consumption when receiving the portion $p_n(1-\mu_1^n-\mu_2^n)F$ from gateway G. Hence, the satellite bandwidth consumption is

$$B(\mu_{\mathbf{1}},\mu_{\mathbf{2}}) = \sum_{n=1}^{N} p_n(2-2\mu_1^n-\mu_2^n)F. \tag{8}$$

Increasing the caching portions at the ground station and/or satellite can reduce the bandwidth consumption.

5 Cache Placement Design

The cached contents are placed into caches C_1 and C_2 via satellite uplink and downlink transmissions during off-peak hours. In this section, the cached portion μ_1^n of all N files at ground station G_s and μ_2^n portion at satellite S are optimized in order to balance the average SDP and bandwidth consumption (maximizing the SPD and minimizing the bandwidth consumption). Hence, this optimization problem is formed as the following a bi-objective optimization problem:

$$\text{minimize}\,(-w\cdot\psi(\mu_{\mathbf{1}},\mu_{\mathbf{2}}) + (1-w)\cdot B(\mu_{\mathbf{1}},\mu_{\mathbf{2}})) \tag{9}$$

$$\text{subject to} \quad \sum_{n=1}^{N}\mu_1^n\cdot F \le C_1, \quad \sum_{n=1}^{N}\mu_2^n\cdot F \le C_2 \tag{10a}$$

$$\sum_{n=1}^{N} p_n(2-2\mu_1^n-\mu_2^n)F \le B_{S-max} \tag{10b}$$

$$0 \le \mu_1^n+\mu_2^n \le 1 \text{ with } n=1,2,...,N \tag{10c}$$

where $w \in (0,1)$ is a non-negative weight representing the performance important between SDP and bandwidth consumption. A larger value of w means the amount of cached content is decided in favour of having a higher SDP and vice versa. The set of constraints (10a) ensures that the cached contents will not exceed the cache size of C_1 and C_2. Constraint (10b) makes sure that the bandwidth consumption stays within the satellite bandwidth capacity B_{S-max}. Constraint (10c) shows the nature of partial content of all files caching scheme.

Eq. (9) can be solved using the genetic algorithm described in [11]. We omit the details of the genetic algorithm here for brevity.

6 Numerical Results

In this section, numerical results are presented for two different caching policies in terms of system average SDP and satellite bandwidth consumption. The

results are compared between the proposed two-tier cache system and the single-tier cache system adopted from [2,9,13]. The caching policy for single-tier cache system is corresponding to the policy cached at ground station in the two-tier case.

Uniform Caching Policy: All of N files are cached with the same portion $\hat{\mu_1}$ at the satellite and $\hat{\mu_2}$ at the ground station. In uniform caching, we have $\mu_{\mathbf{1}} = [\hat{\mu_1}, \hat{\mu_1}, ..., \hat{\mu_1}]$ and $\mu_{\mathbf{2}} = [\hat{\mu_2}, \hat{\mu_2}, ..., \hat{\mu_2}]$ where $0 < \hat{\mu_1} + \hat{\mu_2} < 1$.

Popular Caching Policy: The most popular files are cached with a larger portion at the ground station and a smaller portion at the satellite. In popular caching, we have $\mu_{\mathbf{1}} = [\eta\hat{\mu}_1^1, \eta\hat{\mu}_1^2, .., \eta\hat{\mu}_1^k, 0, ..., 0]$ and $\mu_{\mathbf{2}} = [\hat{\mu}_1^1, \hat{\mu}_1^2, .., \hat{\mu}_1^k, 0, ..., 0]$ where $\eta \in \mathbb{Z}$, $0 < \eta\hat{\mu}_1^i + \hat{\mu}_1^i < 1$ $(i = 1, 2, ..., k)$ and $\hat{\mu}_1^1, ..., \hat{\mu}_1^k$ follows popular file distribution.

The values for key parameters [8] used in this section are presented in Table 1. Because it is required to have more than $100\,dB$ of SIC for FD system to achieve the same signal-to-noise-ratio-plus-interference as that of the HD system [10], we choose the SIC quality parameter $\beta = 0.0001$ for most of our system configuration under FD transmission. With this value of β, the SIC is achieved from $110\,dB$ to $120\,dB$. The fading states for the satellite-terrestrial links are defined by $\{m_1, b_1, \Omega_1\} = \{5, 0.251, 0.279\}$ and $\{m_2, b_2, \Omega_2\} = \{4, 0.126, 0.835\}$ [7] when approaching average shadowing. End-users are randomly distributed inside a circle with radius $10\,km$ and center at G_s.

Table 1. Parameters used for numerical results

Parameter	Value	Parameter	Value
N	500 files	F	100 Mb
α	0.8	β	0.0001
B_{m-n}/B_{S-G_s}	2/10 Gb	$P_S/P_G/P_{G_s}$	10/30/2 W
$B_{G_s-U_i}$	2 Gb	σ^2	-120 dBm/Hz
d_{S-G_s}/d_{G-S}	35,786 km	α_s/α_g	2/3

We first investigate the effect of percentage of file cached at ground station μ_1 under uniform caching policy. With 10 end-users, the numerical results are shown in Fig. 2. The total caching capacity in Fig. 2 is C_1 for single-tier cache system and $C_1 + C_2$ for two-tier cache system. For both single-tier/two-tier cache systems, the average SDP increases with more percentage of content cached at ground station (Fig. 2(a)). The satellite bandwidth consumption consumes more in single-tier cache system (Fig. 2(b)). It is observed from Fig. 2 that achieving better average SDP with less satellite bandwidth consumption happens in single-tier cache system when μ_1 is no more than 50%. In two-tier cache system, the caching strategy is still effective as long as μ_1 is less than 55%; Otherwise, caching more content will not improve the system performances.

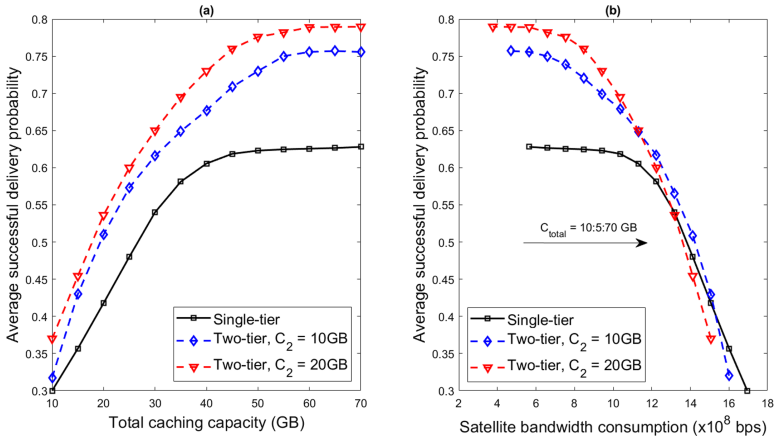

Fig. 2. Two-tier vs. single-tier systems under uniform caching.

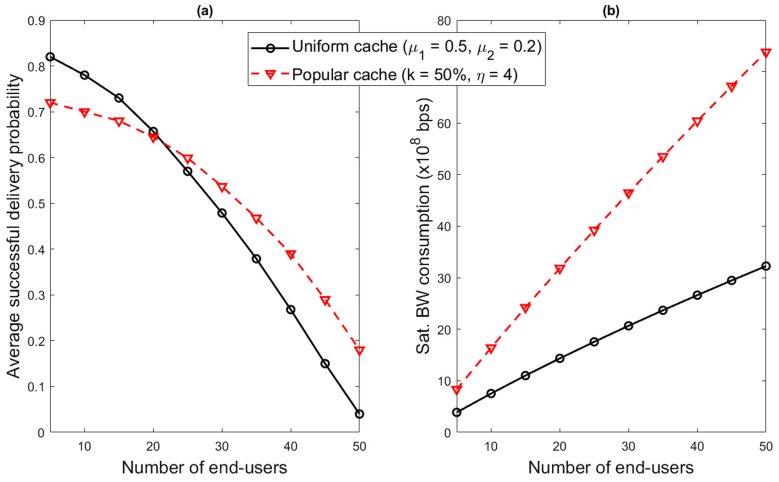

Fig. 3. Two-tier network capacity.

Secondly, we study the two-tier cache system capacity under uniform and popular caching policies. Under uniform caching policy, 50% of each file are prefetched at the ground station and 20% at the satellite. For popular caching policy, the threshold $k = 0.5$ meaning one half of N files are cached and the ratio of percentage cached at the two layers is $\eta = 4$. As shown in Fig. 3(a), the more ground users, the smaller average SDP for both caching policies. For less than 20 users, the uniform caching policy outperforms the popular one. Otherwise, its SDP is surpassed by that of the popular caching policy. Figure 3(b) shows the satellite bandwidth consumption. As serving more users, the popular caching case consumes more bandwidth than the uniform caching case. This result is

caused by the amount of data transmitted in satellite uplink/downlink when a requested file is not cached due to its popularity.

7 Conclusion

In this paper, we study the performance of a two-tier cache aided full-duplex satellite-terrestrial network on two metrics: the successful delivery probability and the satellite bandwidth consumption. Both metrics are investigated with their performances presented via numerical results under uniform caching and popular caching policies. Depending on the system use cases, the optimal cache placement scheme can be chosen in order to achieve better average SDP and less satellite bandwidth consumption.

Acknowledgment. This work was supported by the La Trobe University Postgraduate Research Scholarship, the La Trobe University Full-Fee Research Scholarship, and the Net Zero Scholarship sponsored by Sonepar/SLS.

References

1. Abdi, A., Lau, W.C., Alouini, M., Kaveh, M.: A new simple model for land mobile satellite channels: first- and second-order statistics. IEEE Trans. Wireless Commun. **2**(3), 519–528 (2003)
2. An, K., Li, Y., Yan, X., Liang, T.: On the performance of cache-enabled hybrid satellite-terrestrial relay networks. IEEE Wirel. Commun. Lett. **8**(5), 1506–1509 (2019)
3. Bhatnagar, M.R., Arti, M.K.: Performance analysis of AF based hybrid satellite-terrestrial cooperative network over generalized fading channels. IEEE Commun. Lett. **17**(10), 1912–1915 (2013)
4. Breslau, L., Cao, P., Fan, L., Phillips, G., Shenker, S.: Web caching and Zipf-like distributions: Evidence and implications. In: IEEE Conference on Computer Communications Societies (INFOCOM), NY, USA, pp. 126–134 (1999)
5. Dinesh, B., Sachin, K.: Fastforward: fast and constructive full duplex relays. In: Proceedings of the 2014 ACM Conference on SIGCOMM (SIGCOMM 2014), IL, USA, pp. 199–210 (2014)
6. Gradshteyn, I.S., Ryzhik, I.M.: Tables of Integrals, Series and Products, 6th ed. (2000)
7. Guo, K., et al.: On the performance of the uplink satellite multiterrestrial relay networks with hardware impairments and interference. IEEE Syst. J. **13**(3), 2297–2308 (2019)
8. HughesNet: Echostar xix satellite (2020). https://www.hughesnet.com/whats-new/satellite-launch
9. Kalantari, A., Fittipaldi, M., Chatzinotas, S., Vu, T.X., Ottersten, B.: Cache-assisted hybrid satellite-terrestrial backhauling for 5g cellular networks. In: 2017 IEEE Global Communications Conference (GLOBECOM), Singapore, pp. 1–6 (2017)
10. Li, H., et al.: Self-interference cancellation enabling high-throughput short-reach wireless full-duplex communication. IEEE Trans. Wirel. Commun. **17**(10), 6475–6486 (2018)

11. Li, J., Balazs, M.E., Parks, G.T., Clarkson, P.J.: A species conserving genetic algorithm for multimodal function optimization. Evol. Comput. **10**(3), 207–234 (2002)
12. Paschos, G.S., Iosifidis, G., Tao, M., Towsley, D., Caire, G.: The role of caching in future communication systems and networks. IEEE J. Sel. Areas Commun. **36**(6), 1111–1125 (2018)
13. Vu, T.X., Maturo, N., Vuppala, S., Chatzinotas, S., Grotz, J., Alagha, N.: Efficient 5G edge caching over satellite. In: 36th International Communications Satellite Systems Conference (ICSSC 2018), pp. 1–5 (2018)
14. Vural, S., Navaratnam, P., Wang, N., Wang, C., Dong, L., Tafazolli, R.: In-network caching of internet-of-things data. In: 2014 IEEE International Conference on Communications (ICC), Sydney, Australia, pp. 3185–3190 (2014)
15. Wu, H., Li, J., Lu, H., Hong, P.: A two-layer caching model for content delivery services in satellite-terrestrial networks. In: 2016 IEEE Global Communications Conference (GLOBECOM), DC, USA, pp. 1–6 (2016)